



## **Risky future for Mediterranean forests unless they undergo extreme carbon fertilization**

Guillermo Gea-Izquierdo, Antoine Nicault, Giovanna Battipaglia, Isabel Dorado-Liñán, Emilia Gutiérrez, Montserrat Ribas, Joel Guiot

### **► To cite this version:**

Guillermo Gea-Izquierdo, Antoine Nicault, Giovanna Battipaglia, Isabel Dorado-Liñán, Emilia Gutiérrez, et al.. Risky future for Mediterranean forests unless they undergo extreme carbon fertilization. Global Change Biology, Wiley, 2017, 23 (7), pp.2915-2927. 10.1111/gcb.13597 . insu-02269704

**HAL Id: insu-02269704**

**<https://hal-insu.archives-ouvertes.fr/insu-02269704>**

Submitted on 23 Aug 2019

**HAL** is a multi-disciplinary open access archive for the deposit and dissemination of scientific research documents, whether they are published or not. The documents may come from teaching and research institutions in France or abroad, or from public or private research centers.

L'archive ouverte pluridisciplinaire **HAL**, est destinée au dépôt et à la diffusion de documents scientifiques de niveau recherche, publiés ou non, émanant des établissements d'enseignement et de recherche français ou étrangers, des laboratoires publics ou privés.

**Risky future for Mediterranean forests unless  
they undergo extreme carbon fertilization**

**Running head:** Mediterranean forests, climate change and CO<sub>2</sub>

<sup>1</sup>G Gea-Izquierdo, <sup>2</sup>A Nicault, <sup>3,4</sup>G Battipaglia, <sup>1</sup>I Dorado-Liñán, <sup>5</sup>E, Gutiérrez, <sup>5</sup>M Ribas, <sup>6</sup>J Guiot

<sup>1,7</sup>INIA-CIFOR. Ctra. La Coruña km. 7.5 28040 Madrid, Spain. <sup>2</sup>Aix-Marseille

Université/CNRS FR 3098 ECCOREV 13545 Aix-en-Provence, France. <sup>3</sup>Department of Environmental, Biological and Pharmaceutical Sciences and Technologies<sup>[SEP]</sup>Second

University of Naples<sup>[SEP]</sup>Via Vivaldi, 43 - 81100 Caserta, Italy. <sup>4</sup>Ecole Pratique des

Hautes Etudes (PALECO EPHE), Institut des Sciences de l'Evolution, University of

Montpellier 2, F-34090 Montpellier, France. <sup>5</sup>Departament <sup>4</sup>Departament d'Ecologia,

Universitat de Barcelona, Avda. Diagonal 643, 08028 Barcelona, Spain. <sup>6</sup>Aix-Marseille

Université/CNRS/IRD UM 34, CEREGE 13545 Aix-en-Provence. <sup>7</sup>Corresponding

author: phone 0034913471461; email gea.guillermo@inia.es

**Abstract**

Forest performance is challenged by climate change but higher atmospheric [CO<sub>2</sub>] (c<sub>a</sub>) could help trees mitigate the negative effect of enhanced water stress. Forest projections using data-assimilation with mechanistic models are a valuable tool to assess forest performance. Firstly, we used dendrochronological data from 12 Mediterranean tree species (6 conifers, 6 broadleaves) to calibrate a process-based vegetation model at 77 sites. Secondly, we conducted simulations of gross primary production (GPP) and radial growth using an ensemble of climate projections for the period 2010-2100 for the high-emission RCP8.5 and low-emission RCP2.6 scenarios. GPP and growth projections were simulated using climatic data from the two RCPs combined with: (i) expected c<sub>a</sub>;

(ii) constant  $c_a = 390$  ppm, to test a purely climate-driven performance excluding compensation from carbon fertilization. The model accurately mimicked the growth trends since the 1950s when, despite increasing  $c_a$ , enhanced evaporative demands precluded a global net positive effect on growth. Modeled annual growth and GPP showed similar long-term trends. Under RCP2.6 (i.e. temperatures below  $+2^\circ\text{C}$  with respect to preindustrial values) the forests showed resistance to future climate (as expressed by non-negative trends in growth and GPP) except for some coniferous sites. Using exponentially growing  $c_a$  and climate as from RCP8.5, carbon fertilization overrode the negative effect of the highly constraining climatic conditions under that scenario. This effect was particularly evident above 500 ppm (which is already over  $+2^\circ\text{C}$ ), which seems unrealistic and likely reflects model miss-performance at high  $c_a$  above the calibration range. Thus, forest projections under RCP8.5 preventing carbon fertilization displayed very negative forest performance at the regional scale. This suggests that most of western Mediterranean forests would successfully acclimate to the coldest climate change scenario but be vulnerable to a climate warmer than  $+2^\circ\text{C}$  unless the trees developed an exaggerated fertilization response to  $[\text{CO}_2]$ .

**Keywords:** Dendroecology; process-based models; carbon fertilization; climate change; MAIDEN; water stress; forest dynamics.

**Type of paper:** Original research article

## Introduction

Future climate will trigger changes in ecosystem functioning, including enhancement in forest vulnerability to water stress (Giorgi & Lionello 2008; van der Molen *et al.* 2011; Anderegg *et al.* 2015). Understanding how forests will respond to warmer conditions but under higher than present  $c_a$  is crucial to assess future forest performance. Theoretically, plants should enhance growth and net primary productivity (NPP) by optimization of different functional traits in response to elevated  $[CO_2]$  (i.e.  $c_a$  levels way above present values,  $eCO_2$ ) if this was a limiting factor. In practice, rising  $c_a$  has enhanced intrinsic water-use efficiency (iWUE) in forests but this was not generally translated on a net increase of growth, meaning that other factors such as water stress and/or nutrient limitation have overridden the potential positive effect of  $CO_2$  (Peñuelas *et al.* 2011; Keenan *et al.* 2013; Reichstein *et al.* 2013; van der Sleen *et al.* 2014; Kim *et al.* 2016).

The net effect on tree growth of the interaction 'Climate x  $CO_2$ ' can depend nonlinearly on  $c_a$  levels (Reichstein *et al.* 2013). Observational data show evidence up to current  $c_a < 403$  ppm whereas future emission scenarios project  $c_a$  far above this level (IPCC 2014). Free-Air Carbon dioxide Enrichment (FACE) experiments were designed to address this issue. In these experiments  $[CO_2]$  was elevated up to 600-800 ppm but they were carried out under current environmental conditions mostly on temperate forests (Battipaglia *et al.* 2013; De Kauwe *et al.* 2013; Baig *et al.* 2015; Kim *et al.* 2016; Norby *et al.* 2016). Thus, the effect of  $eCO_2$  on forest performance in relation to climate and other environmental factors needs to be addressed in other biomes where more constraining (warmer and drier) conditions are expected for the future (Giorgi & Lionello 2008; García-Ruiz *et al.* 2011; IPCC 2014). The role that  $CO_2$  could play to compensate the negative impact of increasing water stress on forests has long been



71 debated. Plants can coordinate different functional traits in response to eCO<sub>2</sub> and  
72 drought-prone species at dry sites could benefit more from eCO<sub>2</sub> (Medlyn & De Kauwe  
73 2013; Duursma *et al.* 2016; Kelly *et al.* 2016). Leaf-level responses are easier to predict  
74 than canopy or ecosystem-level responses (Fatichi *et al.* 2015). Consequently, there is  
75 still uncertainty on how the forest carbon cycle will adjust in the future because multiple  
76 interactive factors determine the net response of forests at different scales (Breda *et al.*  
77 2006; Niinemets 2010; van der Molen *et al.* 2011; Kattge *et al.* 2011).

78 Vegetation models combine the effect of different stress factors on different  
79 functional traits to achieve a proper understanding of forest functioning. These models  
80 should be able to combine C-sink and C-source limitations to provide key information  
81 on how forests will develop in the future (Sala *et al.* 2012; McDowell *et al.* 2013;  
82 Fatichi *et al.* 2014; Anderegg *et al.* 2015; Walker *et al.* 2015). There is a constant need  
83 to improve the representation of hydrological, physical and biological processes in  
84 models. In addition, improvement of model performance needs to be achieved through  
85 benchmarking and data-assimilation (Peng *et al.* 2011; Pappas *et al.* 2013; Medlyn *et al.*  
86 2015; Prentice *et al.* 2015). Dendrochronological data have long been used to assess  
87 empirical relationships between climate and growth, which can be used as an indicator  
88 of tree fitness and performance (Fritts 1976). Process-based models can take into  
89 account the influence of CO<sub>2</sub> on plant functional acclimation. Thus they can help to  
90 reduce uncertainty in growth projections but need continuous feedback from multiproxy  
91 data to ensure realism (Guiot *et al.* 2014; Walker *et al.* 2015). Dendrochronological  
92 records can be used to improve complex process-based models and help to assess forest  
93 dynamics under global change (Babst *et al.* 2014). Assessing forest dynamics is  
94 particularly challenging in ecosystems like those under Mediterranean climate (Morales  
95 *et al.* 2005) where two stress periods (cold in winter and drought in summer) limit plant

performance. Warmer winters could enlarge the growing season and promote higher photosynthetic rates (just in evergreens) but also higher respiration rates, whereas warmer summers would exert a negative impact (higher water stress) on forests. Modeling the net effect on trees of the balance between these two periods is critical to assess the future forest response to climate change.

We analyzed the effect that forthcoming changes in climate and  $c_a$  will yield over Mediterranean forests, which are expected to face a high vulnerability to future climate (Giorgi & Lionello 2008; García-Ruiz *et al.* 2011; IPCC 2014). We calibrated a stand mechanistic model using a network of tree-ring growth chronologies including an ensemble of species covering a wide ecological and geographic range to ensure realism and biological robustness when simulating future forest performance at the regional scale under different climate and  $c_a$  scenarios. C-assimilation and C-allocation were explicitly controlled by climate and  $CO_2$  at different phenological stages (Misson 2004; Gea-Izquierdo *et al.* 2015). Importantly, the model includes a C storage pool to take into account carry-over effects and its daily scale can fit different limiting environmental conditions at different periods within and among years (Sala *et al.* 2012; Fatichi *et al.* 2014). Thus, the net effect in response to the winter and summer stress periods was explicitly assessed. Forest projections were implemented using two contrasting representative concentration pathways (RCPs, van Vuuren *et al.* 2011). Using model simulations of future forest growth and GPP we addressed the following questions: (i) what will be the net effect of a warmer climate for Mediterranean forests?; (ii) to what extent could rising  $c_a$  help compensate the expected negative effect of climate warming on forest growth and productivity? (iii) how will Mediterranean forests perform in relation to the maximum temperature threshold for future climate (i.e. +2.0°C respect to preindustrial levels) agreed in the COP21 (<http://www.cop21paris.org/>)?

## Material and Methods

### *Forest sites: growth data for model calibration*

To calibrate the model at the regional scale we used dendrochronological data from 77 forest sites including 12 Mediterranean tree species: 6 conifers and 6 broadleaves (App. 1). These data were either owned by the authors or obtained from databases (ITRDB, <https://www.ncdc.noaa.gov/data-access/paleoclimatology-data/datasets/tree-ring>; DendroDB, <https://dendrodb.eccorev.fr/framedb.htm>). We explored the data to avoid chronologies where major site disturbances could have affected the decadal-to-multidecadal growth variations. The chronologies included were older than 80 years in order to avoid the effect of juvenile growth (data used for calibration started in 1950) and ended later than 1995. Exceptionally, some sites ending before 1995 in Algeria were included to ensure enough data from that region. The resulting calibration period slightly differed across sites due to the different time-span of chronologies, but always fell between 1950 and 2010 and was greater than 40 years. For the analysis, ring-width growth data were transformed to basal area increments (BAI,  $\text{cm}^2 \text{ year}^{-1}$ ). One output from the model is C allocated to the tree stem ( $\text{g C m}^{-2} \text{ year}^{-1}$ ). To make BAI and model output comparable for model calibration both data were normalized to unitless indices (Misson 2004; Gaucherel et al. 2008).

### *Climate and $c_a$ : historical data and future scenarios*

Daily precipitation and temperature data used for model calibration for 1950-2010 were either obtained from <http://www.meteo.unican.es/datasets/spain02> (Herrera *et al.*, 2012) for Spain (20 km grid) or from <http://hydrology.princeton.edu/data.php> (Sheffield *et al.* 2006) for the rest ( $1^\circ$  grid). Data were downscaled to match mean climatic local

values where these were available. For the future forest projections we used two greenhouse gas (GHG) radiative forcing scenarios developed for the Fifth Report of the IPCC (IPCC 2014), called RCPs (Van Vuuren *et al.* 2011). RCP8.5 (GHGRF<8.5 W/m<sup>2</sup>) is the “business as usual” scenario. RCP2.6 is the most optimistic and stringent among RCPs, corresponding to strong mitigation policies with a GHG radiative forcing constrained to remain <2.6 W/m<sup>2</sup>. RCP2.6 is the only RCP limiting global warming to +2°C relative to the pre-industrial level. We used a multimodel ensemble of 19 simulations for RCP2.6 and 18 simulations for RCP8.5 performed by 13 climatic institutes (see App. 2). The global climate models have a coarse resolution, from one to more than five degrees depending on the model. There is often some mismatch between the stand level and input climatic data (Körner 2003; Potter *et al.* 2013; Pappas *et al.* 2015). This was minimized as possible by downscaling climate scenarios to match the shared period of the historical data. Under RCP8.5 the projected climate for our study sites describes a relative increase in mean annual temperature (MAT) of +5.0°C and a decrease of over 40% in mean annual precipitation (MAP) by 2100 respect to current values. Under RCP2.6 the projected climate forecasts a mean increase in MAT of +1.0°C by 2068, stabilizing thereafter, with no decrease in MAP respect to current conditions (App. 3).

#### *The process-based model MAIDEN*

The vegetation model MAIDEN (Fig. 1) was originally developed to be used with dendrochronological data by being calibrated to both time series of radial growth and estimates of transpiration from sap-flow experiments (Misson 2004). Recently, the model has been further developed to be used with evergreen Mediterranean taxa with a multiproxy approach using gross primary productivity (GPP) estimates from Eddy

covariance stations and plot growth data (Gea-Izquierdo *et al.* 2015). Inputs are daily climatic data (precipitation, maximum and minimum temperatures) and  $c_a$ . In addition

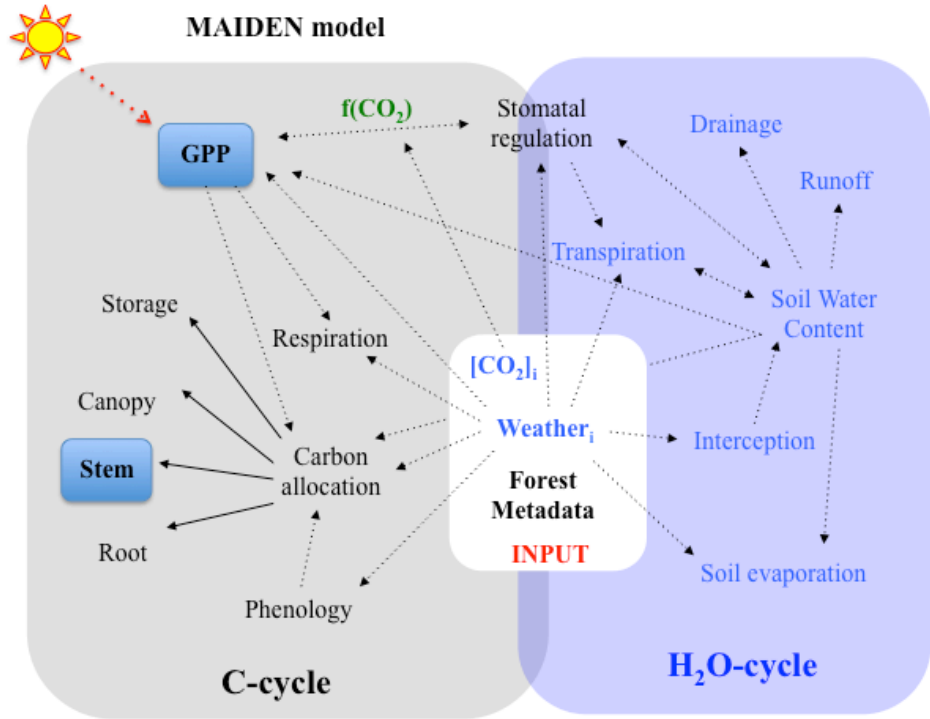


Fig. 1. Outline of MAIDEN. Only GPP (gross primary production) and biomass allocated to the stem (used to calibrate the model sitewise) estimates (blue boxes) are reported along the manuscript. Daily output of each variable is generated based on the input data of day  $i$ . ‘Weather’ corresponds to daily integrals of precipitation as well as maximum and minimum daily temperatures. GPP and ‘Stomatal conductance’ are functions of  $CO_2$ , whereas variability within the other processes is mostly driven by meteorological inputs directly or indirectly (e.g. SWC). For more details on the functions and processes outlined see Misson (2004) and Gea-Izquierdo *et al.* (2015).

the model requires as input different site related physiographic characteristics and species functional traits (see Gea-Izquierdo *et al.* 2015 for details). The processes within the model are mainly functions of climate,  $CO_2$  and soil water availability (hence water

stress). The model acts at the stand level calculating carbon and water fluxes (Fig. 1) using a coupled photosynthesis-stomatal conductance model. It uses the standard biochemical model of Farquhar *et al.* (1980) in which photosynthesis is driven by the most limiting between Rubisco-limited activity and electron-transport. Stomatal conductance is also estimated using a widely used equation as a function of vapor pressure deficit (VPD, Leuning 1995). After GPP and autotrophic respiration have been estimated carbon is allocated to different tree components. Photosynthesis and allocation are driven by decoupled non-linear (daily) functions of climate. Thus growth is not only a direct function of C availability and the model is designed to address in time not only C-source but also C-sink limitations, which is an important step required to achieve more robust and realistic vegetation models (Muller *et al.* 2011; Sala *et al.* 2012; Fatichi *et al.* 2014). The model is particularly sensitive to water stress by implicitly modeling as functions of climate and water stress some functional and demographic traits such as leaf area, carbon allocation, leaf- and canopy-level photosynthesis and transpiration (Muller *et al.* 2011; Gea-Izquierdo *et al.* 2015; Duursma *et al.* 2016; Kelly *et al.* 2016). [CO<sub>2</sub>] only affects photosynthesis and stomatal conductance, i.e. leaf area or respiration are direct functions of climate but not CO<sub>2</sub>. A brief outline of the model is shown in Fig. 1.

#### *Model calibration and ecological coherence of the parametric space*

Calibration of complex multiparametric models is necessary to improve model performance and because of the presence of collinearities between parameters and absence of an exact solution (Prentice *et al.* 2015). To ensure good model performance, it is important to assess the functional coherence of parameters to be calibrated. In addition to calibration, it is desirable to run independent validations particularly when

models are fitted for prediction purposes. Nevertheless, we could not run an independent crossvalidation for two reasons: (1) we calibrated against annual growth (i.e. we had a number of observations between 40 and 60) estimates by integrating annually the daily estimates from the model, therefore our data was too short to be split in two, (2) a jackknife was intractable both computationally and also because continuous (daily) time data series are needed to run the model, i.e. in case individual years were left out the model could not calculate the carbon and water dynamics needed to compute the complete time series at each site.

We implemented a species-specific approach rather than using plant functional types (PFTs) as it is often applied in ecosystem models (Kattge *et al.* 2011; Atkin *et al.* 2015; Pappas *et al.* 2016). We applied the model at the regional scale and to different species to analyze forest performance under future climate and  $c_a$ . Data-assimilation was used to apply the model to different ecological conditions and species (Peng *et al.* 2011; Medlyn *et al.* 2015). Overall, the growth data did not show a positive trend whereas  $c_a$  increased steadily in the calibration period (1951-2010). Therefore, by calibrating the model site-wise using non-detrended (but normalized) growth data and observed  $c_a$  levels we assured that the model excluded an artificial carbon fertilization effect on past growth. Additionally, to avoid overestimation of photosynthesis and get unbiased simulations (Schaefer *et al.* 2012), we ensured that maximum GPP daily integrals yielded within ranges given in Baldocchi *et al.* (2010): 4-6 g C m<sup>-2</sup> day<sup>-1</sup> for evergreens and of 10-14 g C m<sup>-2</sup> day<sup>-1</sup> for deciduous species. Similarly, we constrained annual GPP and NPP estimates to be within those measured for similar ecosystems (see Table 3 in Falge *et al.* 2002 and Table 3 in Luyssaert *et al.* 2007). Species Specific leaf area (SLA) was obtained from Mediavilla *et al.* (2008) and Kattge *et al.* (2011).

Here, within the processes in Fig. 1 we show those functions with parameters involved in the calibration phase. For more details, we refer to the original model in Misson (2004) and the updated modified last version in Gea-Izquierdo *et al.* (2015).

$$(i) \quad \theta_g(i) = \frac{1}{1 + \exp(\text{soil}_b \cdot (SWC(i) - \text{soil}_{ip}))} \quad [E1]$$

$$(ii) \quad a_{31}(i) = (1 - \exp(p_{3moist} \cdot SWC(i)) \cdot \left( \exp\left(-0.5 \cdot \left(\frac{T_{max}(i) - p_{3temp}}{p_{3sd}}\right)^2\right) \right) \quad [E2]$$

$$(iii) \quad a_{32}(i) = (1 - \exp(st_{3moist} \cdot SWC(i)) \cdot \left( \exp\left(-0.5 \cdot \left(\frac{T_{max}(i) - st_{3temp}}{st_{3sd\_temp}}\right)^2\right) \right) \quad [E3]$$

$$(iv) \quad a_4(i) = (1 - \exp(st_{4temp} \cdot T_{max}(i)) \cdot \left( \exp\left(-0.5 \cdot \left(\frac{SWC(i)}{st_{4sd\_moist}}\right)^2\right) \right) \quad [E4]$$

$\theta_g$  is a soil water stress function affecting stomatal conductance.  $a_{31}$ ,  $a_{32}$  and  $a_4$  are allocation functions for two different phenological periods (3 and 4).  $a_{31}$  is related to the leaves and  $a_{32}$  to the stem, whereas  $a_4$  determines C allocation between the stem and storage. SWC is soil water content and  $T_{max}$  is daily maximum temperature. We calibrated  $\text{soil}_{ip}$  from [E1];  $p_{3moist}$  and  $p_{3temp}$  from [E2];  $st_{3moist}$  and  $st_{3temp}$  from [E3]; and  $st_{4sd\_moist}$  and  $st_{4temp}$  from [E4]. The rest of parameters were set following Gea-Izquierdo *et al.* (2015). All parameters except  $\text{soil}_{ip}$  (which is related to the stomatal response) help to define carbon allocation in relation to soil water content and air temperature during the active period.

We calibrated these model parameters taking into account variability in functional traits and the response to climate of plant processes related to site and species. To address the local phenotypic response of species (Montwé *et al.* 2016), some of those parameters ( $\leq 7$ ) described in the previous paragraph were calibrated site-wise using maximum likelihood principles and a global optimization algorithm (Gaucherel *et al.* 2008; Gea-Izquierdo *et al.* 2015). A maximum of 7 allocation parameters from [E1] to [E4] were optimized depending on species by comparing normalized annual integrals of



modeled C allocation to the stem and normalized annual growth series. We calculated different statistics to check the goodness of fit: the coefficient of determination ( $R^2$ ), the linear correlation ( $\rho$ ), and the correlation ( $r_{low}$ ) between filtered (using splines with a 50% frequency cutoff of 30 years) observed and modelled growth.  $r_{low}$  was calculated to analyse the model capability to mimic the interannual and decadal growth trends. To discuss the validity of our modelling exercise and since we could not run an independent verification to the calibration conducted, coherence of the intersite multiparametric space was analysed by exploring the ecological significance of parameters compared to different site characteristics including latitude, longitude, altitude, precipitation, temperature, and Penman-Monteith potential evapotranspiration (PET), which was calculated for each site following Allen *et al.* (1998). The relationship between the 7 model parameters fitted at each of the 77 sites and the mean site ecological covariates was explored through pointwise correlations: (i) using site individual indices; (ii) using the principal components (PCs) of the 7 x 77 matrix (Legendre & Legendre 1998).

#### *Forest performance under climate change and different $c_a$ scenarios*

Once the model had been calibrated we implemented forest projections at the 77 sites using simulated climatic data generated under RCP2.6 and RCP8.5. To discuss the effect of  $c_a$  on the net response of forests to climate change we compared two type of forest simulations driven by the multimodel climatic scenarios:

- (i) ‘fertilization’ scenario: with  $c_a$  levels expected for RCP2.6 and RCP8.5.
- (ii) ‘non-fertilization’ scenario: using climate from RCP2.6 and RCP8.5 but constant  $c_a$  = 390 ppm after 2010.

We report GPP in addition to growth projections. Future growth trends were assessed

Group	n	$R^2$		r		$r_{low}$	
		Mean (sd)	Max (Min)	Mean (sd)	Max (Min)	Mean (sd)	Max (Min)
Broadleaves	22	0.343 (0.168)	0.643 (0.0)	0.675 (0.084)	0.821 (0.483)	0.728 (0.185)	0.929 (0.114)
Conifers	55	0.356 (0.141)	0.710 (0.073)	0.676 (0.070)	0.855 (0.537)	0.786 (0.156)	0.968 (0.249)
Total	77	0.353 (0.148)	0.710 (0.0)	0.675 (0.074)	0.855 (0.483)	0.769 (0.165)	0.968 (0.114)

Table 1. Mean values of goodness of fit statistics. n= number of forest sites;  $R^2$ =coefficient of determination; r=coefficient of correlation;  $r_{low}$ =coefficient of correlation of filtered data (see material and methods for details).

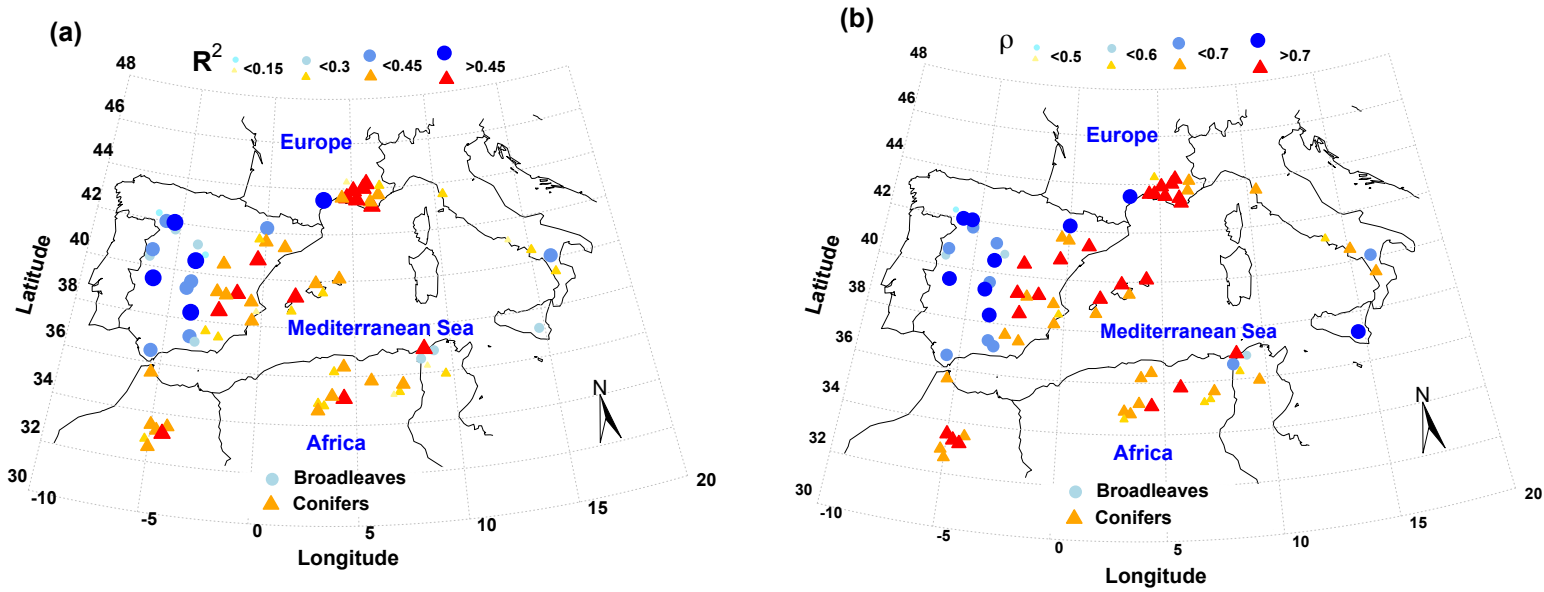


Fig. 2. Map showing the coefficient of determination ( $R^2$ ) and correlation ( $\rho$ ) between dendrochronological data and modeled stem growth data using MAIDEN at the 77 forest sites.  $R^2$  is shown in (a) whereas  $\rho$  in (b). For  $R^2$  we split in four classes:  $0 \leq R^2 < 0.15$ ;  $0.15 \leq R^2 < 0.3$ ;  $0.3 \leq R^2 < 0.45$ ;  $0.45 \leq R^2$ . For  $\rho$  in:  $0.45 \leq \rho < 0.5$ ;  $0.5 \leq \rho < 0.6$ ;  $0.6 \leq \rho < 0.7$ ;  $0.7 \leq \rho$ . Triangles depict conifers, whereas circles broadleaves.

through the slope of simple regressions between simulated growth (or GPP) for a given scenario and site against year for the periods 2010-2100, 2010-2050 and 2051-2100.

## Results

### *Model calibration across western Mediterranean forests*

The model fit against the calibration data is shown in Fig. 2 and Table 1 and the parameters fitted in App. 4. Importantly, data used to calibrate the model did not show an overall significant increase in growth, hence did not suggest evidence of a global net carbon fertilization effect during the last decades (Table 2). The observed growth trends were highly correlated with the model output ( $\rho$  and particularly  $r_{low}$  in Table 1). Correlation between model output (carbon allocated to the stem) and growth data was in average 0.67 whereas mean  $R^2$  was 0.36 (Table 1). The multiparametric space of the 77 fitted models was explored through PCA. The eigenvalues corresponding to the three first principal components (PCs) were over the mean, hence significant according to the Kaiser-Guttman criterion (Legendre & Legendre 1998). These three PCs including the 7 parameters fitted in the calibration phase explained 60.9 % of the variability (PC1 24.7 %, PC2 19.7 % and PC3 16.6%). PC1 was mostly related to parameters linked to humidity: a positive relation with moisture parameters such as  $soil_{ip}$  and  $st_{4sd\_moist}$ , and a negative one with  $st_{3moist}$  (not shown). PC2 was mostly related to parameters linked to temperatures: positively with  $st_{4temp}$  and negatively with  $p_{3temp}$  and  $st_{3temp}$ . PC3 was positively correlated with the humidity parameter  $p_{3moist}$  (not shown). The 77 parameters and the PCs (2 and 3) showed some significant relationships with the site ecological characteristics (Fig.3). Most of the site-based relationships between the fitted parameters and the ecological characteristics of the 77 sites were linked to site temperatures (Fig. 3), whereas almost no significant relationships were found with the

other tested covariates (e.g. site precipitation or PET). These relationships suggest the existence of some ecological coherence within the parametric space fitted for the 77 forest sites, which would support the robustness of the model parameterization used.

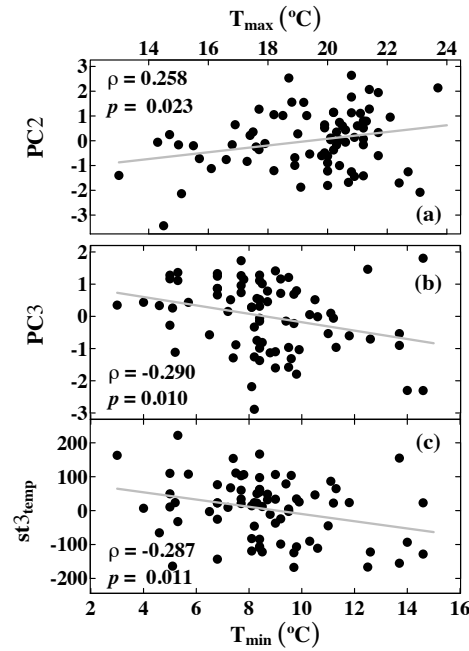


Fig. 3. Ecological coherence of model parameters at the 77 forest sites (only those relationships that were significant are shown): (a) PC2 and site  $T_{\max}$ ; (b) PC3 and site  $T_{\min}$ ; (c)  $st3_{\text{temp}}$  and site  $T_{\min}$ .

### *Growth-GPP projections under changing climate and $c_a$*

The model allocates carbon to different plant compartments driven by different non-linear functions of environmental variability, hence it allows some decoupling between GPP, NPP and secondary growth. In this sense, 59% and 80% of the simulations presented correlations between GPP and growth higher than 0.5 for RCP2.6 and RCP8.5, respectively (App. 5). Thus the majority of sites showed a good agreement between interannual GPP and growth (i.e. generally the modeled interannual variability of growth was driven by that of GPP). Furthermore, the growth trends (long-term, multiannual) were of similar sign (positive, negative or neutral) as those of GPP (Table

Group	Observed past Growth		Growth projections 2010-2099							
			Allowing fertilization (i.e. predicted $c_a$ )				No fertilization (i.e. $c_a = 390$ ppm)			
			GPP		Growth		GPP		Growth	
			2010-2050	2051-2099	2010-2050	2051-2099	2010-2050	2051-2099	2010-2050	2051-2099
Broadleaves	0.79 (0.96)	RCP2.6	0.60 c (2.03)	-0.62 c (0.38)	0.35 b (0.71)	-0.24 d (0.16)	-2.2 a (2.75)	0.26 a (0.47)	-0.65 b (0.89)	0.08 a (0.18)
Conifers	0.17 (0.71)		0.78 c (1.98)	-0.98 d (1.42)	0.14 c (0.31)	-0.08 c (0.13)	-3.64 b (3.92)	-0.02 b (0.82)	-0.34 a (0.38)	0.02 b (0.11)
Total	0.35 (0.83)		0.73 (1.98)	-0.88 (1.22)	0.20 (0.47)	-0.13 (0.16)	-3.21 (3.67)	0.06 (0.74)	-0.43 (0.58)	0.04 (0.13)
Broadleaves	0.79 (0.96)	RCP8.5	2.11 b (2.20)	3.21 b (2.79)	0.93 a (0.96)	1.37 a (1.13)	-4.32 c (3.14)	-5.48 c (2.42)	-1.30 c (1.11)	-1.05 d (0.73)
Conifers	0.17 (0.71)		3.38 a (1.74)	3.75 a (2.51)	0.37 b (0.45)	0.78 b (0.62)	-5.68 d (3.77)	-6.4 d (3.21)	-0.61 b (0.46)	-0.57 c (0.53)
Total	0.35 (0.83)		3.02 (1.96)	3.60 (2.58)	0.53 (0.68)	0.95 (0.83)	-5.29 (3.63)	-6.11 (3.02)	-0.81 (0.77)	-0.71 (0.63)

331

332 Table 2. Growth trends as estimated by the slopes of linear regressions between growth (slopes in  $\text{cm}^2 \cdot \text{year}^{-2}$ ) or GPP (slopes in  $\text{g C m}^{-2} \text{ year}^{-2}$ )

333 and year. Mean slopes are shown for observed past growth and for projected growth and GPP for the periods 2010-2050 and 2051-2099.

334 Standard deviations are between parentheses. One-way ANOVA differences between broadleaves and conifers (RCP2.6 and RCP85, i.e. 4 levels)

335 within columns are depicted with different letters.

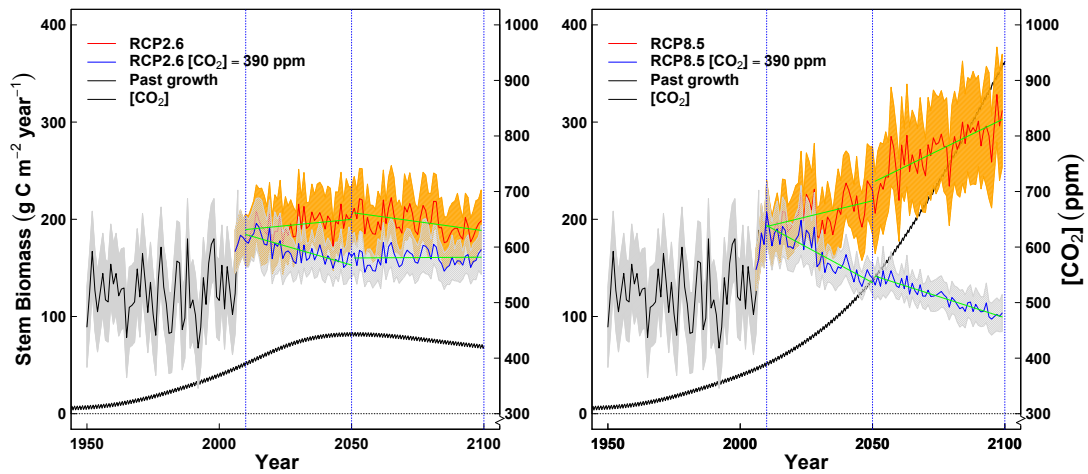


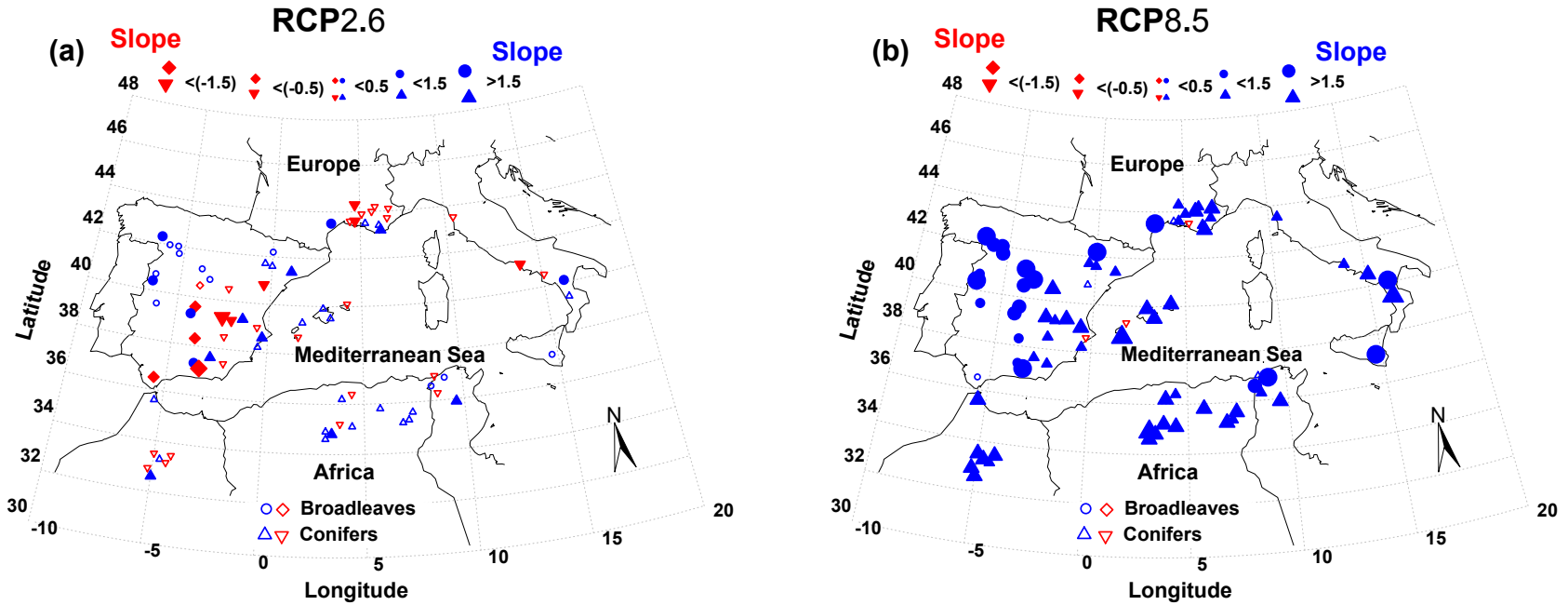
Fig. 4. Example of growth projections at one *Quercus pyrenaica* site (QUPY3 in App.1). Trends (i.e. linear regressions between mean growth and year) for 2010-2050, and 2051-2099 are shown with green lines for the ‘fertilization’ (red line) and ‘non-fertilization’ (blue line) scenarios. These trends correspond to the slopes reported in Table 2, Fig. 5 and Fig. 6. Shaded areas behind annual mean growth values ( $\hat{y}$ ; thick black line is mean past growth) correspond to the confidence intervals for the mean calculated as  $\hat{y} \pm 1.96 \cdot sd_{\hat{y}}/\sqrt{n}$  ( $sd_{\hat{y}}$  is the combined standard deviation of the model estimates and the variability among climatic scenarios;  $n$  is sample size).  $c_a$  values ( $[CO_2]$ ) corresponding to the two scenarios considered (i.e. RCP2.6, RCP8.5) are shown as thin black lines.

2). GPP projections exhibited steeper trends (both positive and negative) for Mediterranean conifers (all evergreen species), whereas the growth trends were steeper for broadleaves (mostly deciduous) than for conifers (Table 2). An example of a model simulation and how the reported trends (i.e. slopes) were calculated is depicted in Fig. 4. Model simulations yielded the greatest GPP and growth in more mesic sites, as expected (App. 6).

According to our projections forest growth would not be much altered when assuming the low emission RCP2.6 scenario with predicted  $c_a$  (Fig. 5). Under the  $c_a$  pathway from RCP2.6, which reaches the  $c_a$  maximum (446 ppm) in 2051, the model simulates a slight increase in growth up to 2050 followed by a slight decrease (Table 2). The resulting overall trend up to 2100 depends on site conditions: most forests exhibited non-significant or reduced trends under RCP2.6 for both  $c_a$  scenarios (Fig. 5, 6). However, for the ‘non-fertilization’ scenario, model simulations suggested significant negative growth trends for some coniferous sites e.g. in Southern France and Eastern Spain (Fig. 6). Therefore the results of the model mostly suggested that forests would acclimate at the regional scale to the climate proposed by RCP2.6. Yet, negative local impacts for some coniferous species would pop up when constraining the carbon fertilization effect.

Climate simulations under RCP8.5 forecast a much warmer scenario with less precipitation than RCP2.6 (App. 3). In response, forest growth projections under this scenario showed a different picture to that described for RCP2.6. For the ‘non-fertilization’ scenario (i.e. constant 390 ppm) future forest growth trends would be negative across all the western Mediterranean. Both conifers and broadleaves would suffer huge decreases in GPP and growth concurrent with the increase in PET expected under RCP8.5. These negative trends were much steeper than those for RCP2.6 (Table 2) and in some cases converged towards zero. In contrast, under the coherent  $c_a$  pathway (exponential increase in  $c_a$  to 935 ppm in 2100) for RCP8.5, the model suggested that plants would not only compensate the more stressing climate but also that growth and GPP would be enhanced across the study region regardless of species (Fig. 6; Table 2).

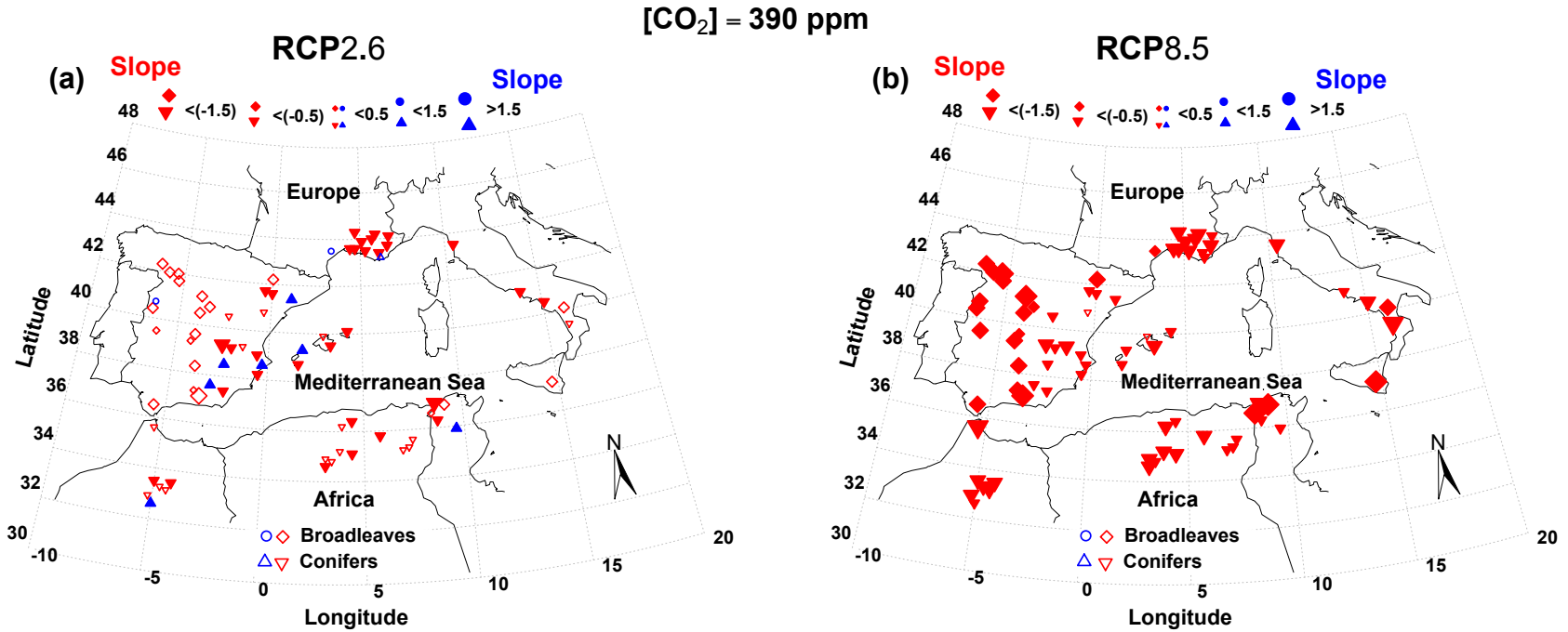
In average RCP8.5 predicts for the studied area in average a +2°C warmer climate (with  $c_a$  = 504 ppm) and a slight MAP reduction by 2050 (App. 3) compared to present



379

380 Fig. 5. Future growth simulations trends using climatic scenarios RCP2.6 (a) and RCP8.5 (b), with predicted (increasing)  $c_a$  between 2010 and  
 381 2099. Trends are estimated as the slopes of the linear regressions between stem biomass growth and year (see Fig. 4). Symbols are scaled as a  
 382 function of the slope value. Red symbols correspond to negative trends whereas blue symbols to positive trends. Solid symbols correspond to  
 383 significant trends ( $\alpha=0.05$ ) whereas empty symbols to non-significant trends.





384  
 385 Fig. 6. Future growth simulations trends between 2010 and 2099 using climatic scenarios RCP2.6 (a) and RCP8.5 (b), with constant  $c_a = 390$   
 386 ppm. Trends are estimated as the slopes of linear regressions between stem biomass growth and year (see Fig. 4). Symbols are scaled as a  
 387 function of the slope value. Red symbols correspond to negative trends whereas blue symbols to positive trends. Solid symbols correspond to  
 388 significant trends ( $\alpha=0.05$ ) whereas empty symbols to non-significant trends.

values (i.e. +2.8°C compared to preindustrial levels). This is over the reduction goal in greenhouse emissions for COP21 (<http://www.cop21paris.org/>) established below +2°C, which otherwise would be achieved in RCP2.6. Simulations under RCP8.5 suggested a negative impact in growth and GPP of climate unless this was compensated by an exaggerated fertilization effect of eCO<sub>2</sub>. The higher the temperature, the more evident and widespread this negative impact would become (Fig. 5, 6; Table 2). In contrast, when allowing fertilization, the greatest positive growth trends (i.e. a greater net fertilization effect) would arise after 2050 with c<sub>a</sub> levels >500 ppm (Table 2). Growth trends after 2050 were steeper than those before 2050 for the ‘fertilization’ scenario (mean difference 0.42, p<0.001) but not for the ‘non-fertilization’ scenario (mean difference 0.09, p=0.403). This highlights the larger influence in simulated growth and GPP of eCO<sub>2</sub> (positive) compared to that of expected high temperatures (negative).

## Discussion

### *Forest future in a warmer western Mediterranean region: what is the role of c<sub>a</sub>?*

Trees can enhance productivity and modify some anatomical and physiological traits (e.g. iWUE) in response to eCO<sub>2</sub> but it is not known how they will perform under future climate and c<sub>a</sub> (Medlyn & De Kauwe 2013; Duursma *et al.* 2016; Kelly *et al.* 2016). A positive net effect of eCO<sub>2</sub> on trees can be hampered by the limiting effect of other environmental constraints such as nitrogen (N) availability and water stress (De Kauwe *et al.* 2013; Reichstein *et al.* 2013; Fernández-Martínez *et al.* 2014; Walker *et al.* 2015; Kim *et al.* 2016). A positive feedback of eCO<sub>2</sub>, e.g. in leaf area (if a steady-state has not been achieved yet; Körner 2006) and NPP, has been reported under current climate conditions in temperate forests where non-climatic factors such as N availability were limiting (Medlyn *et al.* 2015; Walker *et al.* 2015; Kim *et al.* 2016). In contrast,

Duursma *et al.* (2016) did not observe any change in leaf area in response to eCO<sub>2</sub> when leaf area was limited by water availability (i.e. like in our model). Therefore, depending on the most limiting factor, different ecosystems seem to express different responses to eCO<sub>2</sub> under current climatic conditions.

As reflected by our model during the observational period (see Gea-Izquierdo *et al.* 2015 for iWUE), the effect of recent rising  $c_a$  has generally produced an enhancement in iWUE but not in growth rates (e.g. Peñuelas *et al.* 2011; Keenan *et al.* 2013; Saurer *et al.* 2014; van der Sleen *et al.* 2014). Furthermore, studies reporting past growth enhancement within the last 150 years (e.g. at species-specific high-elevation sites) did not consider  $c_a$  as the main factor triggering that growth increase (Salzer *et al.* 2009; Gea-Izquierdo & Cañellas 2014). According to our results, most Mediterranean forests would mitigate the optimistic RCP2.6 scenario either with or without C-fertilization. Hence, forests would mostly endure the +2°C warming limit set within the Paris' Agreement (<http://www.cop21paris.org/>). In contrast, projections under high-emission RCP8.5 would forecast big changes in forest performance. Simulations reflected a very negative impact of climatic conditions under RCP8.5 and a non-fertilization scenario, whereas they suggested a dominant positive effect of eCO<sub>2</sub> at the regional scale (particularly for  $c_a > 500$  ppm) when allowing fertilization even under the very limiting climatic conditions of RCP8.5. The observed positive trends following a Temperature x eCO<sub>2</sub> interaction were not unexpected, because the Farquhar model ensures large direct responses to eCO<sub>2</sub> since Rubisco-limited photosynthesis responds fast to enhanced  $c_a$  (Reichstein *et al.* 2013; Friend *et al.* 2014; Baig *et al.* 2015; Walker *et al.* 2015; Norby *et al.* 2016). Yet, this fertilization effect both for GPP and growth under RCP8.5 looks unrealistic (Körner 2006; Friend *et al.* 2014; Baig *et al.* 2015; Kelly *et al.* 2016).

The future long-term response of forests is uncertain but we expected no positive net effect of eCO<sub>2</sub> on plant growth under very strong water-limitations (van der Molen *et al.* 2011; Girardin *et al.* 2012; Baig *et al.* 2015). Nevertheless, this was only reflected for RCP8.5 by the non-fertilization scenario. Photosynthesis is a saturating function of intercellular CO<sub>2</sub> (Kelly *et al.* 2016) and according to Körner (2006) saturation is expected at levels similar to those of RCP8.5 in 2100 (circa 1000 ppm). Likely, the model does not downregulate assimilation enough under high c<sub>a</sub> or underestimates the limiting effect of other interacting factors (e.g. light, nutrients, water stress, hydraulics) on e.g. maximum carboxylation. This was addressed empirically by setting a limit at 390 ppm but a more detailed understanding of the physiological processes in relation to eCO<sub>2</sub> would definitely help to improve model forecasts. A global negative response of Mediterranean forests to intense warming unless there is an exaggerated C-fertilization effect is, thus, evident in our results. Importantly, this implies negative consequences for forest performance and means that a positive effect of milder winters (e.g. earlier growing season or enhanced winter assimilation in evergreens) would not counteract the negative effect of longer stressing summers. There is an ample debate on the actual factors causing tree death, but it seems that a combination of interrelated C-related traits, hydraulically-related features and climate-related impacts of biotic agents should govern the forest decline and mortality processes (Sala *et al.* 2012; McDowell *et al.* 2013; Aguadé *et al.* 2015; Anderegg *et al.* 2015). Regardless of the final causal factor/s, steep negative growth trends like those under RCP8.5 and no-fertilization strongly suggest changes in stand dynamics and composition and ultimately enhanced mortality at some sites (Bigler *et al.* 2006; van der Molen *et al.* 2011; Gea-Izquierdo *et al.* 2014).

*Forest growth projections under climate change and eCO<sub>2</sub>: utilities and uncertainties*

Models need continuous refinement to achieve robustness, reliability and realism (Prentice et al. 2015). Forecasts of tree growth are a valuable tool to understand forest performance under climate change but there are many sources of uncertainty within model performance and data-assimilation that need discussion (Friend et al. 2014). Caveats in models include: (i) current knowledge of the physiological processes; (ii) model implementation and parameterization (including scale-dependent constraints); (iii) uncertainty of model outputs outside the calibration range (Pappas *et al.* 2013; Prentice *et al.* 2015). Additionally, changes in plasticity of functional traits and plant acclimation processes can bias model projections (Muller et al. 2011). We assumed uniformitarianism (i.e. temporal invariance of the modeled relationships) in model projections but it could be that threshold related responses arise after the calibration boundaries are surpassed. In this sense (iii) is minimized by explicitly modeling processes but not eliminated as a result of (i) and (ii). Despite inherent limitations in models and observational data (Babst *et al.* 2014), by using data-assimilation we maximized the likelihood of getting unbiased past long-term trends to increase reliability of growth projections (Peng *et al.* 2011; Medlyn *et al.* 2015). Forest productivity was analyzed assuming present steady-state stand conditions (e.g. composition, leaf area, root mass) constrained by water stress (Körner 2006). This could bias the analysis of forest dynamics (Körner 2003; Friend et al. 2014; Pappas *et al.* 2015), particularly for mixed stands (Pappas et al. 2013). However, our aim was to analyze performance of the present stands under future environmental conditions, with emphasis on species long-term trends. Changes in inter-species dynamics are away from the scope of our analysis and need to be studied complementary.

The model does not include nutrient dynamics but focuses on the water and carbon cycles and the effect of water stress at different functional levels. This is because

nutrient availability is generally considered secondary in Mediterranean ecosystems compared to water stress, which in addition is expected to increase in the future (Giorgi & Lionello 2008; García-Ruiz *et al.* 2011; IPCC 2014). Thus, the limiting effect of factors such as availability of N, P, or hydraulic constraints could invalidate a C fertilization effect on net growth under eCO<sub>2</sub> (Körner 2006; Norby *et al.* 2010; Fatichi *et al.* 2014; Fernández *et al.* 2014; Friend *et al.* 2014; Baig *et al.* 2015). Our model is simpler than ecosystem models including nutrient and stand dynamics (e.g. Reichstein *et al.* 2013; Walker *et al.* 2015). However, our scale is finer (stand, species-specific compared to PFTs) and, most important, it is driven by actual growth data to ensure unbiased estimation of short- and long-term trends. Other factors such as differences in carry-over effects between conifers and broadleaves, changes in species composition and demography, competition and tree-related traits such as ontogeny and size, partly modulate the forest response to climate (van der Molen *et al.* 2011). However, long-term stand productivity seems to change slightly under moderate disturbances such as those produced by silvicultural treatments or insect infestation (Vesala *et al.* 2005; Amiro *et al.* 2010). Therefore, we believe that climate effects are dominant and the reported long-term trends are robust in relation to variability within these other factors, which would affect mostly in the short-term. The model fit reported was in the range of that in similar studies (Misson 2004; Li *et al.* 2014; Gea-Izquierdo *et al.* 2015; Girardin *et al.* 2016). Different goodness-of-fit at different sites could result on differences in model performance. However, in App. 7A we show how variability in R<sup>2</sup> did not influence the estimated trends (future projections). Particularly, when the trees exhibited long-term trends in the past (observational period), these showed a very high agreement with the modeled growth trends (App. 7B; Table 1). As mentioned, the robustness of our approach relies on the spatial (regional) scale where the model was applied, which

expands model implementation at a broader scale than that where it was previously applied (Misson *et al.* 2004; Gaucherel *et al.* 2008; Gea-Izquierdo *et al.* 2015).

Model simulations can be improved by better addressing the influence of CO<sub>2</sub> on variability of different plant traits (Kattge *et al.* 2011; Atkin *et al.* 2015; Pappas *et al.* 2016). Leaf photosynthesis is negatively affected by drought through several mechanisms including changes in stomatal and mesophyll conductance or reductions in biochemical efficiency (Flexas *et al.* 2005). Both photosynthesis and stomatal conductance were modeled as direct functions of CO<sub>2</sub>. However, warming and increasing water stress in relation to eCO<sub>2</sub> could differently affect autotrophic respiration and photosynthetic capacity, or enhance photorespiration more than photosynthesis (Baig *et al.* 2015; Girardin *et al.* 2016; Rowland *et al.* 2015; Varone & Gratani 2015). Our model takes into account the short-term acclimation of leaf photosynthesis and stomatal conductance to CO<sub>2</sub>, while respiration is set as a function of temperature and GPP (Gea-Izquierdo *et al.* 2015). Different sources of interspecific variability under eCO<sub>2</sub> in autotrophic respiration not explained by models (Atkin *et al.* 2015) or other factors such as species-specific variability in  $J_{\max}/V_{c\max}$  could partly impair our results. Trees modify other traits such as leaf area and sapwood area to withstand xericity (Breda *et al.* 2006; Martin-StPaul *et al.* 2013; Duursma *et al.* 2016; Kelly *et al.* 2016). In our model, intra-annual, inter-annual and long-term structural acclimation of leaf area and allocation rules rely on climate and SWC but not on CO<sub>2</sub>. Thus, addressing the influence of CO<sub>2</sub> on leaf area dynamics by setting SLA and allocation rules also as functions of CO<sub>2</sub> could also help to better assess whether the reported fertilization effect is unrealistic (Duursma *et al.* 2016; Medlyn *et al.* 2015).

In summary, modeled forest growth reflected the observed absence of an overall net positive effect of enhanced  $c_a$  under increased temperatures (i.e. PET) in the recent past.

According to model projections, western Mediterranean forests would mostly mitigate the negative effect of a climate remaining below the maximum warming levels (+2°C) agreed in COP21 (i.e. scenario RCP2.6) but the situation would be very different above those levels (as represented by RCP8.5). Our results suggest that fertilization could override the negative effect of stressing climatic conditions under high-emission RCP8.5 but this fertilization effect of eCO<sub>2</sub> looks unrealistic according to the literature, being most likely a result of miss-performance of models way above the calibration  $c_a$  levels. Consequently, simulations precluding fertilization under high-emission scenarios show very negative forest performance at the regional scale in the future for both conifers and broadleaves. Our results suggest that western Mediterranean forests would not resist the stressing conditions of a much warmer climate unless species exhibited an exaggerated C fertilization effect. It is necessary to include  $c_a$  variability in forest models but it is not enough. We still need a better understanding of the physiological processes governing the capacity of acclimation of different plant traits (e.g.  $V_{cmax}$ ) to the interaction between water stress, eCO<sub>2</sub> and nutrient availability. In this sense, our simulations precluding a fertilization effect seems more realistic than those allowing fertilization under  $c_a$  levels way above those used to calibrate models. Our study provides a comprehensive data-driven analysis of the likely performance of western Mediterranean forests under predicted climate change and  $c_a$ . Yet model performance still needs to be refined under high  $c_a$  as expected in the future.

## Acknowledgements

This study was funded by project AGL2014-61175-JIN of the Spanish Ministry of Economy and Competitiveness and the Labex OT-Med (n° ANR-11-LABEX-0061) from the «Investissements d’Avenir» program of the French National Research Agency



through the A\*MIDEX project (n° ANR-11-IDEX-0001-02). The climate simulations have been extracted from the CMIP5 site (<https://esgf-index1.ceda.ac.uk/projects/esgf-ceda/>) and processed with the help of Romain Suarez.

## References

- Aguadé D, Poyatos R, Gómez M, Oliva J, Martínez-Vilalta J (2015) The role of defoliation and root rot pathogen infection in driving the mode of drought-related physiological decline in Scots pine (*Pinus sylvestris* L.). *Tree Physiology*, **35**, 229–242.
- Allen RG, Pereira LS, Raes D, Smith M (1998) *Crop Evapotranspiration – Guidelines for Computing Crop Water Requirements*, FAO Irrigation and Drainage Paper 56, FAO, 1998, ISBN 92-5-104219-5.
- Amiro BD, Barr AG, Barr JG *et al.* (2010) Ecosystem carbon dioxide fluxes after disturbance in forests of North America. *Journal of Geophysical Research: Biogeosciences*, **115**, G00K02, doi:[10.1029/2010JG001390](https://doi.org/10.1029/2010JG001390).
- Anderegg WRL, Schwalm C, Biondi F *et al.* (2015) Pervasive drought legacies in forest ecosystems and their implications for carbon cycle models. *Science*, **1**, 528–532.
- Atkin OK, Bloomfield KJ, Reich PB *et al.* (2015) Global variability in leaf respiration in relation to climate, plant functional types and leaf traits. *New Phytologist*, **206**, 614–636.
- Babst F, Alexander MR, Szejner P *et al.* (2014) A tree-ring perspective on the terrestrial carbon cycle. *Oecologia*, **176**, 307–322.
- Baig S, Medlyn BE, Mercado LM, Zaehle S (2015) Does the growth response of woody plants to elevated CO<sub>2</sub> increase with temperature? A model-oriented meta-analysis. *Global Change Biology*, **21**, 4303–4319.

588 Baldocchi DD, Ma SY, Rambal S *et al.* (2010) On the differential advantages of  
 589 evergreenness and deciduousness in mediterranean oak woodlands: a flux  
 590 perspective. *Ecological Applications*, **20**, 1583–1597.

591 Battipaglia G, Saurer M, Cherubini P, Calfapietra C, McCarthy HR, Norby RJ, Cotrufo  
 592 MF (2013) Elevated CO<sub>2</sub> increases tree-level intrinsic water use efficiency:  
 593 insights from carbon and oxygen isotope analyses in tree rings across three forest  
 594 FACE sites. *New Phytologist*, **197**, 544–554.

595 Bigler C, Braker OU, Bugmann H, Dobbertin M, Rigling A (2006) Drought as an  
 596 inciting mortality factor in Scots pine stands of the Valais, Switzerland.  
 597 *Ecosystems*, **9**, 330–343.

598 Breda N, Huc R, Granier A, Dreyer E (2006) Temperate forest trees and stands under  
 599 severe drought: a review of ecophysiological responses, adaptation processes and  
 600 long-term consequences. *Annals of Forest Science*, **63**, 625–644.

601 De Kauwe MG, Medlyn BE, Zaehle S *et al.* (2013) Forest water use and water use  
 602 efficiency at elevated CO<sub>2</sub>: a model-data intercomparison at two contrasting  
 603 temperate forest FACE sites. *Global Change Biology*, **19**, 1759–1779.

604 Duursma RA, Gimeno TE, Boer MM, Crous KY, Tjoelker MG, Ellsworth DS (2016)  
 605 Canopy leaf area of a mature evergreen Eucalyptus woodland does not respond to  
 606 elevated atmospheric [CO<sub>2</sub>] but tracks water availability. *Global Change Biology*,  
 607 **22**, 1666–1676.

608 Falge E, Baldocchi D, Tenhunen J *et al.* (2002) Seasonality of ecosystem respiration  
 609 and gross primary production as derived from FLUXNET measurements.  
 610 *Agricultural and Forest Meteorology*, **113**, 53–74.

611 Farquhar GD, von Caemmerer S, Berry JA (1980) A biochemical model of  
 612 photosynthetic CO<sub>2</sub> assimilation in leaves of C<sub>3</sub> species, *Planta*, **149**, 78–90.

- Fatichi S, Leuzinger S, Körner C (2014) Moving beyond photosynthesis : from carbon source to sink-driven vegetation modeling. *New Phytologist*, **201**, 1086–1095.
- Fatichi S, Pappas C, Ivanov VY (2015) Modeling plant-water interactions: an ecohydrological overview from the cell to the global scale. *Wiley Interdisciplinary Reviews Water* 3, 327–368.
- Fernández-Martínez M, Vicca S, Janssens IA et al. (2014) Nutrient availability as the key regulator of global forest carbon balance. *Nature Climate Change*, **4**, 471–476.
- Flexas J, Bota J, Galmes J, Medrano H, Ribas-Carbo M (2006) Keeping a positive carbon balance under adverse conditions: responses of photosynthesis and respiration to water stress. *Physiologia Plantarum*, **127**, 343–352.
- Friend AD, Lucht W, Rademacher TT et al. (2014) Carbon residence time dominates uncertainty in terrestrial vegetation responses to future climate and atmospheric CO<sub>2</sub>. *Proceedings of the Natural Academy of Sciences of the United States of America*, **111**, 3280–5.
- Fritts HC (1976) *Tree Rings and Climate*. Blackburn Press, p. 567.
- García-Ruiz JM, Ignacio Lopez-Moreno J, Vicente-Serrano SM, Lasanta-Martinez T, Begueria S (2011) Mediterranean water resources in a global change scenario. *Earth-Science Reviews*, **105**, 121–139.
- Gaucherel C, Guiot J, Misson L (2008) Evolution of the potential distribution area of french mediterranean forests under global warming. *Biogeosciences*, **5**, 1493–1504.
- Gea-Izquierdo G, Cañellas I. (2014) Contrasting instability in growth trends of Mediterranean oaks at opposite distributional limits. *Ecosystems*, **17**, 228–241.

- Gea-Izquierdo G, Viguera B, Cabrera M, Cañellas I (2014) Drought induced decline could portend widespread pine mortality at the xeric ecotone in managed mediterranean pine-oak woodlands. *Forest Ecology and Management*, **320**, 70–82.
- Gea-Izquierdo G, Guibal F, Joffre R, Ourcival J-M, Simioni G, Guiot J. (2015) Modelling the climatic drivers determining photosynthesis and carbon allocation in evergreen Mediterranean forests using multiproxy long time series. *Biogeosciences*, **12**, 3695-3712.
- Giorgi F, Lionello P (2008) Climate change projections for the Mediterranean region. *Global and Planetary Change*, **63**, 90–104.
- Girardin MP, Bernier PY, Raulier F, Tardif JC, Conciatori F, Guo XJ (2012) Testing for a CO<sub>2</sub> fertilization effect on growth of Canadian boreal forests. *Journal of Geophysical Research-Biogeosciences*, **116**, G01012, doi:[10.1029/2010JG001287](https://doi.org/10.1029/2010JG001287).
- Girardin MP, Hogg EH, Bernier PY, Kurz WA, Guo XJ, Cyr G (2016) Negative impacts of high temperatures on growth of black spruce forests intensify with the anticipated climate warming. *Global Change Biology*, **22**, 627–643.
- Guiot J, Boucher E, Gea-Izquierdo G (2014) Process models and model-data fusion in dendroecology. *Frontiers in Ecology and Evolution*, **2**, 1–12.
- Herrera S, Gutierrez JM, Ancell R, Pons MR, Frias MD, Fernandez J (2012) Development and Analysis of a 50 year high-resolution daily gridded precipitation dataset over Spain (Spain02). *International Journal of Climatology*, **32**, 74-85.
- IPCC (2014) Climate Change 2014: Synthesis Report. Contribution of Working Groups I, II and III to the Fifth Assessment Report of the Intergovernmental Panel on Climate Change [Core Writing Team, R.K. Pachauri and L.A. Meyer (eds.)]. IPCC, Geneva, Switzerland, 151 pp.

- Kattge J, Díaz S, Lavorel S *et al.* (2011) TRY - a global database of plant traits. *Global Change Biology*, **17**, 2905–2935.
- Keenan TF, Hollinger DY, Bohrer G, Dragoni D, Munger JW, Schmid HP, Richardson AD (2013) Increase in forest water-use efficiency as atmospheric carbon dioxide concentrations rise. *Nature*, **499**, 324–7.
- Kelly JWG, Duursma RA, Atwell BJ, Tissue DT, Medlyn BE (2016) Drought x CO<sub>2</sub> interactions in trees: A test of the low-intercellular CO<sub>2</sub> concentration (C<sub>i</sub>) mechanism. *New Phytologist*, **209**, 1600–1612.
- Kim D, Oren R, Qian SS (2016) Response to CO<sub>2</sub> enrichment of understory vegetation in the shade of forests. *Global Change Biology*, **22**, 944–956.
- Körner (2003) Slow in, rapid out - Carbon flux studies and Kyoto targets. *Science*, **300**, 1242–1243
- ST – Slow in, rapid out – Carbon flux s.
- Körner C (2006) Plant CO<sub>2</sub> responses: an issue of definition , time and resource supply. *New Phytologist*, **172**, 393–411.
- Legendre P, Legendre L (1998) *Numerical Ecology*. 853 pp. Elsevier, Amsterdam.
- Leuning R (1995) A critical appraisal of a combined stomatal- photosynthesis model for C<sub>3</sub> plants. *Plant, Cell & Environment*, **18**, 339–355.
- Li G, Harrison SP, Prentice IC, Falster D (2014) Simulation of tree ring-widths with a model for primary production, carbon allocation and growth. *Biogeosciences*, **11**, 6711–6724.
- Luyssaert S, Inglis I, Jung M *et al.* (2007) CO<sub>2</sub> balance of boreal, temperate, and tropical forests derived from a global database. *Global Change Biology*, **13**, 2509–2537.
- Martin-Stpaul NK, Limousin J-M, Vogt-Schilb H, Rodríguez-Calcerrada J, Rambal S, Longepierre D, Misson L (2013) The temporal response to drought in a

Mediterranean evergreen tree: comparing a regional precipitation gradient and a throughfall exclusion experiment. *Global change biology*, **19**, 2413–26.

McDowell NG, Fisher RA, Xu C *et al.* (2013) Evaluating theories of drought-induced vegetation mortality using a multimodel – experiment framework. *New Phytologist*, **200**, 304–321.

Mediavilla S, Garcia-Ciudad a., Garcia-Criado B, Escudero a. (2008) Testing the correlations between leaf life span and leaf structural reinforcement in 13 species of European Mediterranean woody plants. *Functional Ecology*, **22**, 787–793.

Medlyn B, De Kauwe B (2013) Carbon dioxide and water use in forests. *Nature*, **499**, 20–22.

Medlyn BE, Zaehle S, De Kauwe MG *et al.* (2015) Using ecosystem experiments to improve vegetation models. *Nature Climate Change*, **5**, 528–534.

Misson L (2004) MAIDEN: a model for analyzing ecosystem processes in dendroecology. *Canadian Journal of Forest Research*, **34**, 874–887.

Montwé D, Isaac-Renton M, Hamann A, Spiecker H (2016) Drought tolerance and growth in populations of a wide-ranging tree species indicate climate change risks for the boreal north. *Global Change Biology*, **22**, 806–815.

Morales P, Sykes MT, Prentice IC *et al.* (2005) Comparing and evaluating process-based ecosystem model predictions of carbon and water fluxes in major European forest biomes. *Global Change Biology*, **11**, 2211–2233.

Muller B, Pantin F, Génard M, Turc O, Freixes S, Piques M, Gibon Y (2011) Water deficits uncouple growth from photosynthesis, increase C content, and modify the relationships between C and growth in sink organs. *Journal of Experimental Botany*, **62**, 1715–1729.

- Niinemets U (2010) Responses of forest trees to single and multiple environmental stresses from seedlings to mature plants: Past stress history, stress interactions, tolerance and acclimation. *Forest Ecology and Management*, **260**, 1623–1639.
- Norby RJ, Warren JM, Iversen CM, Medlyn BE, McMurtrie RE (2010) CO<sub>2</sub> enhancement of forest productivity constrained by limited nitrogen availability. *Proceedings of the National Academy of Sciences USA*, **107**, 19368–19373.
- Norby RJ, De Kauwe MG, Domingues TF *et al.* (2016) Model-data synthesis for the next generation of forest free-air CO<sub>2</sub> enrichment (FACE) experiments. *New Phytologist*, **209**, 17–28.
- Pappas C, Fatichi S, Leuzinger S, Wolf A, Burlando P (2013) Sensitivity analysis of a process-based ecosystem model: Pinpointing parameterization and structural issues. *Journal of Geophysical Research: Biogeosciences*, **118**, 505–528.
- Pappas C, Fatichi S, Rimkus S, Burlando P, Huber M (2015) The role of local scale heterogeneities in terrestrial ecosystem modeling. *Journal of Geophysical Research: Biogeosciences*, **120**, 341–360.
- Pappas C, Fatichi S, Burlando P (2016) Modeling terrestrial carbon and water dynamics across climatic gradients: Does plant trait diversity matter? *New Phytologist*, **209**, 137–151.
- Peng CH, Guiot J, Wu HB, Jiang H, Luo YQ (2011) Integrating models with data in ecology and palaeoecology: advances towards a model-data fusion approach. *Ecology Letters*, **14**, 522–536.
- Peñuelas J, Canadell JG, Ogaya R (2011) Increased water-use efficiency during the 20th century did not translate into enhanced tree growth. *Global Ecology and Biogeography*, **20**, 597–608.

- Potter KA, Arthur Woods H, Pincebourde S (2013) Microclimatic challenges in global change biology. *Global Change Biology*, **19**, 2932–2939.
- Prentice IC, Liang X, Medlyn BE, Wang YP (2015) Reliable, robust and realistic: The three R's of next-generation land-surface modelling. *Atmospheric Chemistry and Physics*, **15**, 5987–6005.
- Reichstein M, Bahn M, Ciais P *et al.* (2013) Climate extremes and the carbon cycle. *Nature*, **500**, 287–295.
- Rowland L, Lobo-do-Vale RL, Christoffersen BO *et al.* (2015) After more than a decade of soil moisture deficit, tropical rainforest trees maintain photosynthetic capacity, despite increased leaf respiration. *Global Change Biology*, **21**, 4662–4672.
- Sala A, Woodruff DR, Meinzer FC (2012) Carbon dynamics in trees: feast or famine? *Tree physiology*, **32**, 764–75.
- Salzer MG, Hughes MK, Bunn AG, Kipfmüller KF (2009) Recent unprecedented tree-ring growth in bristlecone pine at the highest elevations and possible causes. *Proceedings of the National Academy of Sciences USA*, **106**, 20348–20353.
- Saurer M, Spahni R, Frank DC *et al.* (2014) Spatial variability and temporal trends in water-use efficiency of European forests. *Global change biology*, **20**, 3700–3712.
- Schaefer K, Schwalm CR, Williams C *et al.* (2012) A model-data comparison of gross primary productivity: Results from the North American Carbon Program site synthesis. *Journal of Geophysical Research*, **117**, G03010, doi:10.1029/2012JG001960.
- Sheffield J, Goteti G, Wood EF (2006) Development of a 50-yr high-resolution global dataset of meteorological forcings for land surface modeling. *Journal of Climate*, **19** (13), 3088–3111.



758 Stephenson NL, Das a J, Condit R *et al.* (2014) Rate of tree carbon accumulation  
 759 increases continuously with tree size. *Nature*, **507**, 90–3.  
 760 van Der Molen MK, Dolman AJ, Ciais P *et al.* (2011) Drought and ecosystem carbon  
 761 cycling. *Agricultural and Forest Meteorology*, **151**, 765–773.  
 762 van der Sleen P, Groenendijk P, Vlam M *et al.* (2014) No growth stimulation of tropical  
 763 trees by 150 years of CO<sub>2</sub> fertilization but water-use efficiency increased. *Nature*  
 764 *Geoscience*, **8**, 24–28.  
 765 van Vuuren DP, Edmonds J, Kainuma M *et al.* (2011) The representative concentration  
 766 pathways: An overview. *Climatic Change*, **109**, 5–31.  
 767 Varone L, Gratani L (2015) Leaf respiration responsiveness to induced water stress in  
 768 Mediterranean species. *Environmental and Experimental Botany*, **109**, 141–150.  
 769 Vesala T, Suni T, Rannik Ü *et al.* (2005) Effect of thinning on surface fluxes in a  
 770 boreal forest. *Global Biogeochemical Cycles*, **19**, 1–11.  
 771 Walker AP, Zaehle S, Medlyn BE *et al.* (2015) Predicting long-term carbon  
 772 sequestration in response to CO<sub>2</sub> enrichment: How and why do current ecosystem  
 773 models differ? *Global Biogeochemical Cycles*, **29**, 476–495.

774 App. 1. List of chronologies used and their source. Lat=latitude; Long=longitude; Altit=altitude; MAP = mean annual precipitation; MAT= mean  
775 annual temperature (°C); PET<sub>pm</sub>=Penman-Monteith annual evapotranspiration; P=annual precipitation.

#	Site	Species	Country	Lat (°)	Long (°)	Altit (m)	MAP (mm)	MAT (°C)	PET <sub>pm</sub> (mm)	P-PET (mm)	P/PET	Source
1	QUPY2	<i>Quercus pyrenaica</i> Willd.	Spain	42.2	-6.7	1300	985	9.65	962.4	22.6	1.02	Gea-Izquierdo <i>et al.</i> (2014)
2	QUPY3			41.9	-6.2	760	453.9	12.3	1108.9	-655.0	0.41	
3	QUPY4			40.3	-6.8	900	1135.7	14.1	1213.3	-77.6	0.94	
4	QUPY5			40.7	-3.7	1300	580	10.1	1017.0	-437.0	0.57	
6	QUPY7			39.5	-4.3	900	496.5	14.3	1228.9	-732.4	0.40	
6	QUPY8			38.2	-4.1	890	474	15.0	1356.4	-882.4	0.35	
7	QUPY9			37.2	-4.0	1486	509.8	11.3	1164.8	-655.0	0.44	
8	QUPY10			37.0	-3.7	1550	619.3	9.8	984.5	-365.2	0.63	
9	QUPY11			40.8	-4.2	1056	599.9	10.1	1001.8	-401.9	0.6	
10	QUIL1	<i>Quercus ilex</i> L.	Spain	41.6	-5.6	740	433.8	12.5	1139.7	-705.9	0.38	Gea-Izquierdo <i>et al.</i> (2011)
11	QUIL2			40.6	-6.7	700	562.6	12.9	1220.6	-658.0	0.46	
12	QUIL3			40.4	-4.2	600	516.6	13.3	1169.5	-652.9	0.44	
13	QUIL4			39.4	-6.4	390	544.1	16.1	1269.4	-725.3	0.43	
14	QUIL5			43.2	3.0	270	1009.1	12.8	1001.5	7.6	1.01	
15	QUFG1	<i>Quercus faginea</i> Lam.	Spain	41.9	-5.7	680	453.9	12.3	1107.8	-653.9	0.41	Gea-Izquierdo (Unpublished data)
16	QUFG2			39.2	-4.5	900	496.5	14.3	1231.7	-735.2	0.40	
17	QUFG3			41.5	-0.3	550	326.1	15.3	1272.3	-946.2	0.26	
18	QUPU1	<i>Quercus pubescens</i> Willd.	Italy	37.1	14.4	430	537.1	15.8	964.2	-427.1	0.56	Garfi (2000)
19	QUCE1	<i>Quercus cerris</i> L.	Italy	40.4	15.8	590	767.3	11.2	878.5	-111.2	0.87	Battipaglia (unpublished data)
20	QUCA1	<i>Quercus canariensis</i> Willd.	Spain	36.4	-5.9	330	988.4	16.1	1195.4	-207.0	0.83	Gea-Izquierdo <i>et al.</i> (2010)
21	QUCA5			36.8	8.8	758	649.3	16.5	1319	-669.7	0.49	

22	QUCA6			36.5	8.1	760	625.2	15.9	1338.8	-713.6	0.47	
23	PIN2	<i>Pinus nigra</i> J.F. Arnold	Algeria	36.3	4.1	1560	580	14.8	1201.0	-621.0	0.48	Touchan <i>et al.</i> (2011)
24	PIN15	<i>Pinus heldreichi</i> H.Christ	Italy	39.3	15.9	1430	806.1	12.4	901.1	-95.0	0.89	<a href="https://dendrodb.eccorev.fr/framedb.htm">https://dendrodb.eccorev.fr/framedb.htm</a>
25	PIPI2	<i>Pinus pinaster</i> Ait.	Morocco	35.5	-5.7	900	611.3	16.4	1156.4	-545.1	0.53	Touchan <i>et al.</i> (2011)
26	PIPN1	<i>Pinus pinea</i> L.	Spain	40.4	-2.6	1055	443.3	11.4	1217.1	-773.8	0.36	<a href="https://www.ncdc.noaa.gov/paleo/study/2863">https://www.ncdc.noaa.gov/paleo/study/2863</a>
27	PIPN2			39.1	-1.7	705	379.8	14.0	1269.4	-889.6	0.30	<a href="https://www.ncdc.noaa.gov/paleo/study/2866">https://www.ncdc.noaa.gov/paleo/study/2866</a>
28	PIPN3			39.2	-2.3	720	264.3	14.1	1330.4	-1066.1	0.20	<a href="https://www.ncdc.noaa.gov/paleo/study/2867">https://www.ncdc.noaa.gov/paleo/study/2867</a>
29	PIPN4			39.2	-2.8	700	343.3	14.5	1347.4	-1004.1	0.25	<a href="https://www.ncdc.noaa.gov/paleo/study/2865">https://www.ncdc.noaa.gov/paleo/study/2865</a>
30	PIPN8		Italy	43.4	10.2	10	962.1	15.3	1019.4	-57.3	0.94	<a href="https://www.ncdc.noaa.gov/paleo/study/16755">https://www.ncdc.noaa.gov/paleo/study/16755</a>
31	PIPN9			41.0	13.6	9	571.8	17.7	974.1	-402.3	0.59	Battipaglia <i>et al.</i> (2016)
32	PIHA1	<i>Pinus halepensis</i> Mill.	France	43.1	5.9	420	645.9	14.7	1201.2	-555.3	0.54	Gea-Izquierdo <i>et al.</i> (2015)
33	PIHA2		Tunisia	36.9	8.3	23	630.3	18.7	1283.0	-652.7	0.49	Gea-Izquierdo (unpublished data)
34	PIHA3			36.2	8.4	950	619.8	15.1	1297.7	-677.9	0.48	
35	PIHA4			35.8	9.3	800	542.3	14.7	1322.1	-779.8	0.41	Touchan <i>et al.</i> (2011)
36	PIHA5			34.8	2.8	1380	349.6	14.5	1315.3	-965.7	0.27	
37	PIHA8		Algeria	35.2	6.9	1300	380.8	14.6	1330.3	-949.5	0.29	
38	PIHA9			35.7	5.5	1200	431.2	15.6	1292.6	-861.4	0.33	
39	PIHA10			35.3	7.1	1650	380.8	14.6	1333.9	-953.1	0.29	
40	PIHA11			35.0	4.1	1100	390.2	15.6	1304.3	-914.1	0.30	Safar (1994), Safar <i>et al.</i> (1992)
41	PIHA12			35.1	3.5	1060	417.2	15.4	1304.8	-887.6	0.32	
42	PIHA13			34.7	3.1	1410	350.8	14.3	1305.5	-954.7	0.27	
43	PIHA14			34.7	2.8	1350	350.8	14.3	1306.5	-955.7	0.27	
44	PIHA15		France	35.1	6.6	1450	380.8	14.6	1333.1	-952.3	0.29	
45	PIHA16			44.1	5.6	600	845.3	11.4	916.2	-70.9	0.92	
46	PIHA17			43.5	4.4	190	743.9	14.0	1029.2	-285.3	0.72	Nicault (1999)
47	PIHA18			43.8	4.8	330	788.9	13.2	1004.1	-215.2	0.79	
48	PIHA19			43.4	6.3	300	742.4	13.2	973.0	-230.6	0.76	

49	PIHA20			43.2	5.8	200	713.2	14.6	1015.3	-302.1	0.70	
50	PIHA21			43.7	5.4	170	816.3	11.8	944.8	-128.5	0.86	
51	PIHA22			44.0	6.4	600	1073.5	9.4	816.0	257.5	1.32	
52	PIHA23			43.4	5.0	150	749.1	13.6	986.4	-237.3	0.76	
53	PIHA28			44.2	4.4	350	888	12.2	966.6	-78.6	0.92	
54	PIHA31			43.8	4.1	300	743.6	14.2	1023.0	-279.4	0.73	
55	PIHA32			38.6	-2.6	1000	350.6	14.7	1203.4	-852.8	0.29	
56	PIHA34			37.3	-2.5	1280	287.6	14.7	1311.1	-1023.5	0.22	
57	PIHA35			38.9	-0.9	800	333.7	13.8	1270.0	-936.3	0.26	
58	PIHA36			40.8	-0.7	850	453.3	13.7	1152.7	-699.4	0.39	
59	PIHA37			38.1	-0.8	10	276.2	18.0	998.5	-722.3	0.28	
60	PIHA38			38.5	-0.6	900	380.1	14.2	1194.3	-814.2	0.32	
61	PIHA39			37.5	-3.2	1150	380.6	12.8	1362.8	-982.2	0.28	
62	PIHA40		Spain	41.6	-0.3	500	335.9	14.4	1203.3	-867.4	0.28	Ribas (2006)
63	PIHA41			41.3	0.8	750	304	14.2	1197.8	-893.8	0.25	
64	PIHA42			41.8	-0.7	350	310.2	14.2	1194.5	-884.3	0.26	
65	PIHA43			38.7	1.3	80	362.4	18.2	1177.3	-814.9	0.31	
66	PIHA44			40.0	3.9	0	486.9	16.7	1071.7	-584.8	0.45	
67	PIHA45			39.4	3.0	250	430.5	17.9	1080.0	-649.5	0.4	
68	PIHA46			39.8	2.6	700	548.7	14.3	1228.7	-680	0.45	
69	PIHA47			39.1	1.5	175	327.6	17.1	1303.5	-975.9	0.25	
70	PIHA48		Italy	40.3	14.8	8	711.5	15.1	1000.7	-289.2	0.71	Battipaglia <i>et al.</i> (2014)
71	CEAT1			32.2	-5.5	1920	483	9.9	1255.1	-772.1	0.38	Touchan <i>et al.</i> (2011)
72	CEAT2			33.1	-4.5	2180	526.5	15.2	1266.8	-740.3	0.42	
73	CEAT3	<i>Cedrus atlantica</i> (Endl.) Manetti ex Carrière	Morocco	32.3	-5.3	2100	463.7	12.2	1339.1	-875.4	0.35	Esper <i>et al.</i> (2007)
74	CEAT4			33.2	-5.3	1830	539.4	10.5	1213.3	-673.9	0.44	
75	CEAT5			32.6	-5.0	2200	492.2	13.5	1360.5	-868.3	0.36	

76	CEAT6		32.6	-4.7	2200	492.2	13.5	1360.5	-868.3	0.36	
77	CEAT7	Algeria	36.3	3.6	1520	576.1	14.7	1196.2	-620.1	0.50	Touchan <i>et al.</i> (2011)

776

## 777 References

- 778 Battipaglia G, Strumia S, Esposito A, Giuditta E, Sirignano C, Altieri S, Rutigliano FA (2014) The effects of prescribed burning on *Pinus*  
779 *halepensis* Mill. as revealed by dendrochronological and isotopic analyses. *Forest Ecology and Management*, **334**, 201-208.
- 780 Battipaglia G, Savi T, Ascoli D, Castagneri D, Esposito A, Mayr S, Nardini A. (2016). Effects of prescribed burning on ecophysiological,  
781 anatomical and stem hydraulic properties in *Pinus pinea* L. *Tree physiology* (in press)
- 782 Esper J, Frank DC, Büntgen U, Verstege A, Luterbacher J, Xoplaki E (2007) Long-term drought severity variations in Morocco. *Geophysical*  
783 *Research Letters* 34, doi: 10.1029/2007GL030844.
- 784 Garfi, G. (2000). Climatic signal in tree-rings of *Quercus pubescens* and *Celtis australis* in South-eastern Sicily. *Dendrochronologia* 18, 41-51.
- 785 Gea-Izquierdo G, Cherubini P, Cañellas I. 2011. Tree-rings reflect the impact of climate change on *Quercus ilex* L. along a temperature gradient  
786 in Spain over the last 100 years. *Forest Ecology and Management* 262, 1807-1816.
- 787 Gea-Izquierdo G, Fonti P, Cherubini P, Martín-Benito D, Chaar H, Cañellas I. 2012. Xylem hydraulic adjustment and growth response of  
788 *Quercus canariensis* Willd. to climatic variability. *Tree Physiology* 32, 401-413.

789 Gea-Izquierdo G, Cañellas I. 2014 Contrasting instability in growth trends of Mediterranean oaks at opposite distributional limits. *Ecosystems*  
790 17, 228-241.

791 Nicault A. (1999). Analyse de l'influence du climat sur les variations inter- et intra-annuelles de la croissance radiale du pin d'Alep (*Pinus*  
792 *halepensis* Mill.) en Provence calcaire. Thèse de l'Université d'Aix-Marseille III, 254 p.

793 Ribas M. (2006). Dendroecología de *Pinus halepensis* Mill. en Este de la Península Ibérica e Islas Baleares: Sensibilidad y grado de adaptación a  
794 las condiciones climáticas. PhD dissertation. University of Barcelona. <http://diposit.ub.edu/dspace/handle/2445/35321>

795 Safar W. Serre-Bachet, F. & Tessier L. (1992). Les plus vieux pins d'Alep vivants connus. *Dendrochronologia*, 10, pp. 41-52.

796 Safar W. (1994). Contribution à l'étude dendroécologique du pin d'Alep (*Pinus halepensis* Mill) dans une région semi-aride d'Algérie : l'Atlas  
797 Saharien (Ouled Naïl - Aurès - Hodna). Thèse de l'université d'Aix - Marseille III., 215 p.

798 Touchan, R., K.J. Anchukaitis, D.M. Meko, M. Sabir, S. Attalah, and A. Aloui. (2011) Spatiotemporal drought variability in northwestern Africa  
799 over the last nine centuries. *Climate Dynamics* 37, 237-252.

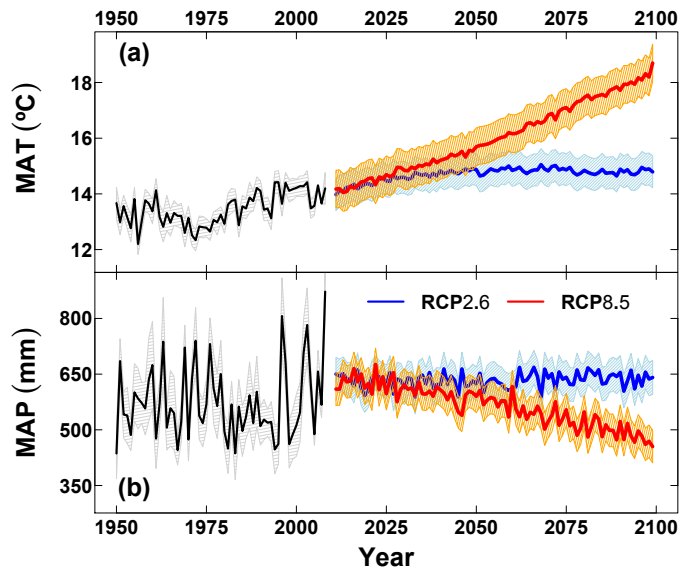
800 App. 2. Model code and Institute of CMIP5 climate simulations included in the study.

801 Crosses indicate when RCP scenarios were selected for a certain Model.

Model	Institute	RCP2.6	RCP8.5
bcc-csm1-1	Beijing Climate Center, China	X	X
bcc-csm1-1-m	Meteorological Administration	X	
BNU-ESM	College of Global Change and Earth System Science, Beijing Normal University	X	X
CanESM2	Canadian Centre for Climate modelling, Canada	X	X
CNRM-CM5	Centre National de Recherches Météorologiques / Centre Européen de Recherche et Formation Avancée en Calcul Scientifique, France	X	X
CSIRO-MK3-6-0	Commonwealth Scientific and Industrial Research Organization in collaboration with Queensland Climate Change Centre of Excellence	X	X
EC-EARTH	EC-EARTH consortium	X	X
FGOALS-g2	LASG, Institute of Atmospheric Physics, Chinese Academy of Sciences and CESS, Tsinghua University	X	X
GFDL-CM3	NOAA Geophysical Fluid Dynamics Laboratory, USA	X	X
GFDL-ESM2G		X	X
GFDL-ESM2M		X	
HadGEM2-ES	Met-Office – Hadley Center, contributed by Instituto Nacional de Pesquisas Espaciais, Spain	X	X
IPSL-CM5A-LR	Institut Pierre-Simon Laplace, France	X	X
IPSL-CM5A-MR		X	X
MIROC-ESM	Japan Agency for Marine-Earth Science and Technology, Atmosphere and Ocean Research Institute (The University of Tokyo), and National MIROC-ESM-CHEM Institute for Environmental Studies	X	X
MIROC-ESM-CHEM		X	X
MIROC5	Atmosphere and Ocean Research Institute (The University of Tokyo), National Institute for MIROC MIROC4h Environmental Studies, and Japan Agency for MIROC5 Marine-Earth Science and Technology	X	X
MPI-ESM-LR	Max-Planck Inst. Für Meteorologie, Germany	X	X
MRI-CGCM3	Meteorological Research Institute, Japan	X	X
NorESM1-M	Norwegian Climate Centre		X
# Simulations		19	18

802

App. 3. Mean daily annual temperature (MAT) and mean annual precipitation (MAP) of the climate model simulations at each of the 77 sites for the RCP 2.6 (a) and RCP 8.5 (b). Shaded areas are confidence intervals at  $\alpha=0.05$  for annual means.





808 App. 4. Mean values and standard deviations of 7 fitted parameters to the 77 sites.  
809

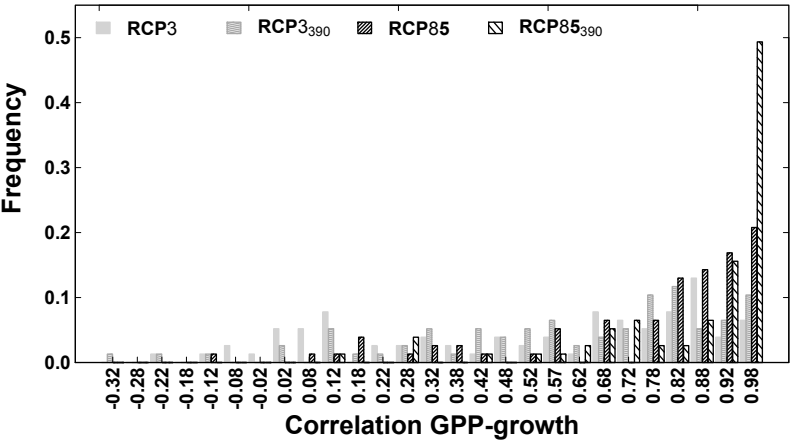
Parameter	Mean	Standard deviation	Minimum	Maximum
soil <sub>ip</sub>	139.0	96.7	3.1	392.9
p <sub>3moist</sub>	-0.255	0.211	-0.700	-0.001
p <sub>3temp</sub>	26.7	77.8	-153.7	181.2
st <sub>3moist</sub>	-0.226	0.197	-0.699	-0.006
st <sub>3temp</sub>	4.8	88.2	-167.4	222.0
st <sub>4sd_moist</sub>	-0.321	0.230	-0.900	-0.009
st <sub>4temp</sub>	334.9	212.2	49.7	1080.2

810

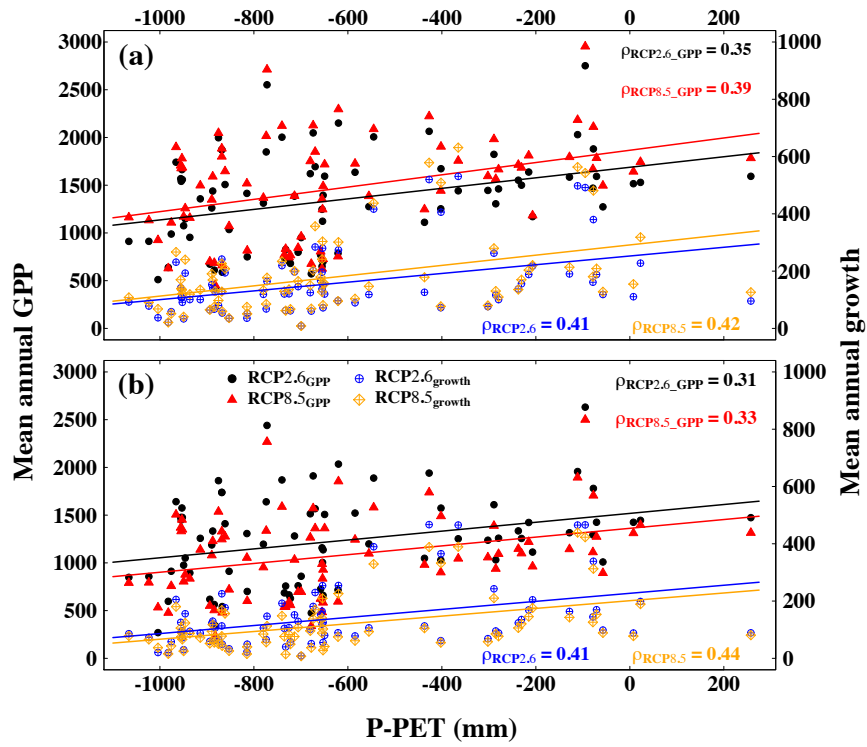
811 App. 5. Distribution of the relationship between GPP and carbon allocation to the stem  
812 (i.e. radial growth) as estimated by a linear correlation.

813

814



815 App.6. Mean projected GPP and growth (2010-2100) and site 'Annual precipitation  
816 minus Penman-Monteith potential evapotranspiration' (P-PET, in mm) for RCP2.6 and  
817 RCP8.5 scenarios: (a) fertilization scenario (i.e. predicted  $c_a$ ); (b) non-fertilization  
818 scenario (i.e.  $c_a=390$  ppm). All relationships ( $\rho$ =correlation) are significant at  $p<0.01$ .



819  
820

821 App. 7. In this figure we show two graphs to support the robustness of our modeling  
 822 approach and the future projections implemented at the regional scale. (A) The  
 823 coefficient of determination ( $R^2$ ) is shown as a function of the projected growth trends  
 824 to demonstrate that there is no relationship between the estimated trends and the  
 825 calibration  $R^2$ . In addition, regardless of  $R^2$ , all projections under RCP8.5 are either  
 826 positive (fertilization, in blue) or negative (non-fertilization, in red), whereas variability  
 827 in RCP2.6 slopes estimated is independent of the goodness of fit (as estimated by  $R^2$ ,  
 828 see (A)). In (B), to illustrate the model capacity to fit the interannual (decadal) growth  
 829 trends, we show the slopes estimated on past growth observations in function of the  $r_{low}$   
 830 statistic (correlations between filtered series).  $r_{low}$  was greater than 0.7 in 73% of the  
 831 models fitted (B). Most importantly,  $r_{low}$  was greater than 0.6 in all cases when there was  
 832 a significant past trend (in (B) we highlight those sites where past  $|\text{slope}| \geq 0.35$   
 833  $\text{cm}^2 \cdot \text{year}^{-2}$ ), which means that the model was able to mimic the long-term growth-trends  
 834 when trees exhibited some positive or negative trend in the past.

